

Posvećeno dr. sc. Franji Ranogajcu za njegov 70. rođendan  
Dedicated to Franjo Ranogajec, Ph.D., on the occasion of his 70<sup>th</sup> birthday

Ivan Šmit,\* Matjaž Denac,\*\* Iztok Švab,\* Gregor Radonjič,

\*Vojko Musil, Tanja Jurkin, Anđela Pustak

Ruđer Bošković Institute, Zagreb, Croatia

\*University of Maribor, FEB Maribor, Institute of Technology, Maribor, Slovenia

\*\*ISOKON, Production and Processing of Thermoplastics, Ltd, Slovenske Konjice, Slovenia

# Structuring of polypropylene matrix in composites

ISSN 0351-187

UDK 678.742

Authors review / Autorski pregled

Received / Primljeno: 6. 7. 2009.

Accepted / Prihvaćeno: 9. 12. 2009.

## Abstract

Binary isotactic polypropylene (iPP) composites with talc and wollastonite were modified with different elastomers: poly(styrene-*b*-butadiene-*b*-styrene) (SBS), poly(styrene-*b*-ethylene-co-propylene) (SEP), poly(styrene-*b*-ethylene-co-butylene-*b*-styrene) (SEBS), SEBS grafted with maleic anhydride (SEBS-*g*-MA), ethylene/propylene/diene terpolymer (EPDM), and propylene-based metallocene (mEPR) at different content ratios and studied by different microscopic techniques (optical, SEM, TEM), wide-angle X-ray diffraction (WAXD) and differential scanning calorimetry (DSC). Complex investigations of the structure-property relationships by comparison of ternary iPP composites with constitutive binary composites and binary blends showed that different factors affect (re)structuring of the semicrystalline polypropylene matrix during its crystallization and solidification during preparation by compression moulding. Structural investigations were focused on determination of influencing factors in crystallite and spherulite growth, phase structure of the iPP crystallites, degree of crystallinity, orientation of filler particles and iPP crystallite, structuring/spherulitization of the iPP matrix, and phase morphology of particles and polypropylene composite and constitutive blend systems. From the interplay of different factors in structuring of the iPP matrix the following influencing factors could be recognized: (i) nucleation by tiny dispersed particles of polymers and filler particles, (ii) orientation of the iPP crystallite and filler particles, (iii) migration/transferring of the iPP chains from melt islands to growing lamellae during solidification, (iv) encapsulation of dispersed/filler particles leading to core-shell morphology, (v) steric hindrance factors generated by filler and dispersed elastomer particles in the spherulitization of the iPP matrix, and (vi) possible partly co-crystallization in the iPP/propylene-based metallocene copolymer (iPP/mEPR) regions.

## KEY WORDS:

core-shell morphology

crystallization

ethylene/propylene/diene rubber

orientation

phase morphology

polymer composites

polymer matrix structuring

polypropylene

propylene-based metallocene copolymers

spherulitization

styrene block copolymers

talc

wollastonite

## KLJUČNE RIJEČI:

etilen/propilen/dienski kaučuk

fazna morfologija

kristalizacija

metalocenski kopolimeri propilena

morfologija jezgra-ljuska

orijentacija

polimerni kompoziti

polipropilen

sferolitizacija

stirenski blok kopolimeritalk

strukturiranje polimerne matrice

talc

wollastonit

## Strukturiranje polipropilenske matrice u kompozitu

### Sažetak

Binarni kompoziti izotaktnog polipropilena (iPP) s talkom i wollastonitom modificirani s različitim elastomerima: (poli(stiren-*b*-butadien-*b*-stiren) (SBS), poli(stiren-*b*-etilen-co-propilen) (SEP), poli(stiren-*b*-etilen-co-butilen-*b*-stiren) (SEBS), SEBS kopolimer cijepljen s maleinskim anhidridom (SEBS-*g*-MA), etilen/propilen/dienski kaučuk (EPDM) i metallocenski kopolimeri polipropilena (mEPR)) pri definiranim različitim omjerima sadržaja proučavani su pomoću različitih mikroskopskih metoda (optička, SEM, TEM), rendgenskom difrakcijom pri velikom kutu (WAXD) i diferencijalnom pretražnom kalorimetrijom (DSC). Kompleksna istraživanja odnosa struktura-svojstvo uspoređivanjem ternarnih iPP kompozita sa sastavnim binarnim kompozitima i binarnim mješavinama pokazala su da različiti čimbenici djeluju na (re)strukturiranje kristalaste polipropilenske matrice tijekom kristalizacije i očvršćivanja (solidifikacije) tijekom pripreme ploča izravnim prešanjem. Strukturna istraživanja usmjerena su na određivanja čimbenika koji utječu na rast kristalita i sferolita, faznu strukturu iPP kristalita, stupanj kristalnosti, orijentaciju čestica punila i iPP kristalita, faznu morfologiju čestica i sustava kompozita i sastavnih mješavina polipropilena. U međuigrri ovih čimbenika koji sudjeluju u strukturiranju iPP matrice mogu se prepoznati slijedeći utjecajni faktori: (i) nukleacija sitnim dispergiranim česticama polimera i punila, (ii) orijentacija iPP kristalita i čestica punila, (iii) migracija/prijenos iPP lanaca iz otočića taljevine u rastuće lamele tijekom očvršćivanja, (iv) uklapanje (enkapsulacija) dispergiranih čestica i punila koja vodi do morfologije jezgra-ljuska, (v) steričkih faktora smetnji koje generiraju čestice punila i dispergirane čestice elastomera pri sferolitizaciji iPP matrice i (vi) moguća djelomična kokristalizacija u područjima iPP/metallocenski kopolimer polipropilena (iPP/mEPR).

## Introduction

One of the most effective areas for spreading polyolefin applications have become particulate-filled polymer composites as engineering plastics materials, which represent the economic venues for tailoring the desired properties and for expanding new products due to favourable cost/performance ratio. Isotactic polypropylene (iPP) is one of the most widely used commodity plastomers due to its outstanding properties, in particular, easy processability, recycling ability, heat distortion temperature above 100°C, versatility of applications, etc. Commonly used mineral fillers for the iPP are talc, calcium carbonate, glass beads and fibres, mica, silica and wollastonite.<sup>1-3</sup>

The incorporation of inorganic filler improves some mechanical properties of the iPP such as stiffness, hardness and strength, but it usually reduces the toughness worsening additionally the poor impact strength of iPP at low temperatures. Additionally, there are difficult areas for nonpolar polyolefin in applications where adhesion, compatibility, wettability, printability, or reactivity are required. Reduced toughness and low interactivity at the iPP-filler interface in composites could be improved by introducing appropriate block or graft copolymer that can play the role of good impact modifier and compatibilizer simultaneously. Accordingly, different elastomers: thermoplastic elastomers of styrenic block copolymers (TPEs SBC – used term in the text SRBC according styrenic rubber block copolymers), ethylene/propylene/diene terpolymer (EPDM), and thermoplastic elastomers of propylene-based metallocene copolymers (mEPR) with propylene being the major component were chosen as impact modifiers and at the same time as compatibilizers for polypropylene/talc (iPP/T) and polypropylene/wollastonite (iPP/W) composites.<sup>4,5</sup>

Tailoring/optimization of mechanical properties of the iPP composites is possible on the basis of understanding their structure-property relationships. Determination of the structure-property relationships of the iPP composites demands complex investigation of structure, morphology, adhesion and mechanical properties depending on complex function composite composition, properties of the components and processing conditions.<sup>6,7</sup> Added polymers and fillers affect ultimate mechanical properties of composites and blends in two ways: (i) they act directly as harder filler particles with determined properties (shape, size, surface and modulus) affecting thus strength, stiffness/hardness, adhesion and abrasion properties,<sup>1-7</sup> and (ii) they affect crystallization processes in polymer matrix and ultimate supermolecular structure of semicrystalline polymer.<sup>3-5</sup> Different factors during solidification of samples may affect/occur in the restructuring of semicrystalline iPP matrix causing different effects (phase nucleation, crystallite and spherulite growth/size, prolonged crystallization, crystallite orientation, morphology, etc.). The restructuring of polymer matrix is mainly investigated as function of nucleation effect of fillers and elastomers and crystallization rate.<sup>8,9</sup>

Complex investigations of the structure-property relationships of the iPP blends and composites have shown that other factors also affect restructuring of the semicrystalline polypropylene matrix during its crystallization/solidification in blending/compounding processes.<sup>4,5</sup> The aim of this article is to present how the addition of fillers (talc, wollastonite) and different copolymers as compatibilizers and/or impact modifiers affects the restructuring of polypropylene matrix determining thus final end-use properties of the iPP composites.

## Experimental part

### Materials

Two types of isotactic polypropylenes (iPP-1, iPP-2), four types of talcs (T-1, T-2, T-3, T-4), five types of wollastonites (W-1, W-2, W-3, W-4, W-5), poly(styrene-*b*-butadiene-*b*-styrene) (SBS), poly(styrene-

*b*-ethylene-*co*-propylene) (SEP), two types of poly(styrene-*b*-ethylene-*co*-butylene-*b*-styrene) (SEBS-1 and SEBS-2), SEBS grafted with maleic anhydride (SEBS-g-MA), ethylene/propylene/diene terpolymer (EPDM), two types of propylene-based metallocene copolymers (mEPR-1, mEPR-2), were used in this work.

Binary composites polypropylene/talc (iPP/T) and polypropylene/wollastonite (iPP/W) composites with volume ratios 100/0, 96/4, 92/8, 88/12 and 84/16 were prepared. Ternary composites were prepared with iPP/filler 96/4, 92/8, and 88/12 volume ratios selected on the basis of results obtained in binary composite systems. Different SRBC elastomers (SBS, SEP, SEBS, SEBS-g-MA), ethylene/propylene/diene terpolymer (EPDM) and two types of propylene-based metallocene copolymers (mEPR-1 and mEPR-2) of 2.5, 5, 10 and 20 vol.% was added to binary iPP/talc or iPP/wollastonite composites. Polymers and fillers characteristics are shown in Table 1.

### Composites preparation

Composites and blends of different compositions were prepared by melt compounding in oil heated Brabender kneading chamber at 200°C for 7 min with the rotor speed of 50 rpm. After finishing the compounding process, they were rapidly transferred into a mould, placed in the preheated hydraulic press at 220°C. Increased load to 100 bar was used and after a defined time the plates were removed and cooled to the room temperature in the air. Compression moulded binary and ternary composites and blends were used for investigations of structure and morphology.

### Testing methods

In order to realize scheduled investigations of the structure-property relationships of binary and ternary iPP composites and blends, the following methods were performed.

#### Optical Microscopy

Thin cross-microtomed sections of the 1-mm-thick plates were examined with a *Leitz Orthoplan* and *Leica* light microscope (*Model DMLS*) with a digital camera at crossed and parallel polars. The maximal anisotropic diameter of the spherulites,  $d_{\max}$ , was measured on several polarization micrographs of each sample, and they were quantified as a number average spherulite diameter,  $d_{\text{sph}}$ .

#### Scanning Electron Microscopy (SEM)

Scanning electron microscope *Jeol JSM-840A* was used for studying the morphology of the investigated blends and composites. The samples were fractured in liquid nitrogen and covered with gold before being examined with the microscope at an acceleration voltage of 10kV. To provide better insight into blend morphology, PS and SRBC elastomers in blends and composites were etched with xylene and mEPR elastomers with *n*-heptane from the sample surface at the room temperature. All SEM micrographs are secondary electron images.

#### Transmission Electron Microscopy (TEM)

Ultrathin sections (75-85nm thick) of the investigated blends and composites were cut from 4-mm thick plate with *Reichert-Jung Ultracut E* microtome equipment with a diamond knife. Before microtoming, composite samples were exposed to OsO<sub>4</sub> vapour for three days in order to contrast and harden the samples. Microtomed ultrathin sections were then placed on copper grids and micrographs were taken at an acceleration voltage of 100 kV by a *Tecnai G<sup>2</sup> 12* microscope with CCD camera (*Gatan Bioscan*).

#### Wide-Angle X-Ray Diffraction (WAXD)

The wide-angle X-ray diffractograms of specimens (1-mm thick plates) were taken by a *Philips* diffractometer with monochromatized CuK<sub>α</sub> radiation in the diffraction range of  $2\theta = 5-40^\circ$ . A degree of crystallinity,  $w_{c,x'}$  was evaluated by the *Hermans-Wei-*

dingler method.<sup>10</sup> The crystallite sizes  $L_{110}$  and  $L_{040}$  were calculated by Scherrer formula.<sup>11</sup>  $B$  value (earlier known as  $K$  value)<sup>12</sup>, as a measure for hexagonal  $\beta$ -form content, as well as orientation parameters  $A_{110}$ ,  $A_{130}$  and  $C$  used as measures for orientations of corresponding (110), (130), and (040) planes were calculated by formula (1) proposed by Zipper *et al.*<sup>13</sup>

#### Differential Scanning Calorimetry (DSC)

The thermal analysis was performed with a *Perkin Elmer* DSC-7 calorimeter. The specimens were cut from 1-mm thick compression

moulded plates, placed in aluminium pans and sealed. The instrument was operated in a dynamic mode. First, the samples were heated to 200°C with a controlled heating rate of 10°C/min in extra pure nitrogen environment and then kept at that same temperature for 5 min. Thermograms were recorded during the cooling cycle with a cooling rate of 5 to 25°C, as well as by second heating cycle to 200°C with a heating rate of 10°C/min. The melting temperatures,  $T_m$ , and enthalpies of melting,  $\Delta h$ , of samples were obtained from the peak on the second melting curve. The crystallinity,  $w_{c,h}$ , of iPP and of the composites was calculated from enthalpy  $\Delta h$  per gram recalculated on iPP mass. The following quantities were given

TABLE 1 - Characteristics of used polymers and fillers

Material	Trade name	Source	Properties
iPP-1	Novolen 1100 L	BASF	$M_n = 47\ 000$ g/mol, $M_w/M_n = 9.3$ MFI = 6.0 g/10min, $\rho = 0.908$ g/cm <sup>3</sup>
iPP-2	Moplen HP501L	Basell	$M_n = 120\ 000$ g/mol, $M_w/M_n = 5.4$ MFI = 6.0 g/10 min, $\rho = 0.90$ g/cm <sup>3</sup> ,
T-1	Naintsch A-20	Luzenac	untreated talc, $\rho = 2.78$ g/cm <sup>3</sup> , $d_{50} = 3.8$ $\mu$ m, specific surface area = 6.5 m <sup>2</sup> /g
T-2	Naintsch A-20 V360	Luzenac	surface treated with 1% of N-(N-benzyl-aminoethyl)-aminopropyl-trimethoxysilane, $\rho = 2.78$ g/cm <sup>3</sup> , $d_{50} = 3.8$ $\mu$ m, specific surface area = 6.5 m <sup>2</sup> /g
T-3	Naintsch A-20 V592	Luzenac	surface treated with 2% of aminopropyl-trimethoxysilane, $\rho = 2.78$ g/cm <sup>3</sup> , $d_{50} = 3.8$ $\mu$ m, specific surface area = 6.5 m <sup>2</sup> /g
T-4	Naintsch A-20 V659	Luzenac	surface treated with 2% of 3-aminopropyl-triethoxysilane, $\rho = 2.78$ g/cm <sup>3</sup> , $d_{50} = 3.8$ $\mu$ m, specific surface area = 6.5 m <sup>2</sup> /g
W-1	Tremin 939 300 ZST	Quarzwerte	treated with combination of silanes $\rho = 2.85$ g/cm <sup>3</sup> , $d_{50\%} = 9$ $\mu$ m, specific surface area = 1.2 m <sup>2</sup> /g
W-2	Tremin 939 300 AST	Quarzwerte	treated with aminosilane $\rho = 2.85$ g/cm <sup>3</sup> , $d_{50\%} = 9$ $\mu$ m, specific surface area = 1.2 m <sup>2</sup> /g
W-3	Tremin 939 300 FST	Quarzwerte	treated with alkylsilane $\rho = 2.85$ g/cm <sup>3</sup> , $d_{50\%} = 9$ $\mu$ m, specific surface area = 1.2 m <sup>2</sup> /g
W-4	Tremin 939 300 PST	Quarzwerte	treated with aminosilane $\rho = 2.85$ g/cm <sup>3</sup> , $d_{50\%} = 10$ $\mu$ m, specific surface area = 1.2 m <sup>2</sup> /g
W-5	Tremin 939 100 AST	Quarzwerte	treated with aminosilane $\rho = 2.85$ g/cm <sup>3</sup> , $d_{50\%} = 13$ $\mu$ m, specific surface area = 0.9 m <sup>2</sup> /g
SBS	Kraton D-1102 CS	Kraton Polymers	$M_n = 67\ 200$ g/mol, $M_w/M_n = 1.70$ MFI = 6.6 g/10min, $\rho = 0.940$ g/cm <sup>3</sup>
SEP	Kraton G-1701	Kraton Polymers	$M_n = 89\ 500$ g/mol, $M_w/M_n = 1.5$ MFI = 0.62 g/10min, $\rho = 0.920$ g/cm <sup>3</sup>
SEBS-1	Kraton G-1651	Kraton Polymers	$M_n = 162\ 300$ g/mol, $M_w/M_n = 1.20$ MFI = n.a.
SEBS-2	Kraton G-1652	Kraton Polymers	$M_n = 65\ 900$ , $M_w/M_n = 1.07$ MFI = 0.5 g/10 min, $\rho = 0.91$ g/cm <sup>3</sup>
SEBS-g-MA	Kraton KG-1901	Kraton Polymers	$M_n = 47\ 300$ g/mol, $M_w/M_n = 1.55$ MFI = 3.1 g/10min, $\rho = 0.91$ g/cm <sup>3</sup>
EPDM	Dutral TER 4038	Montedison	Mooney viscosity ML (1+4) 394 K = 65, $\rho = 0.865$ g/cm <sup>3</sup>
mEPR-1	Vistamaxx VM-1100	Exxon Mobil	$M_n = 92\ 900$ g/mol, $M_w/M_n = 3.4$ MFI = 4.5 g/10min, $\rho = 0.863$ g/cm <sup>3</sup> ,
mEPR-2	Vistamaxx VM-1120	Exxon Mobil	$M_n = 48\ 100$ g/mol, $M_w/M_n = 2.66$ MFI = 20.0 g/10min, $\rho = 0.863$ g/cm <sup>3</sup>

from crystallization exotherm: peak temperature of the crystallization exotherm,  $T_c$ ; slope of the exotherm,  $S_c$ ; temperature of the onset of crystallization,  $T_{onset}$ ; width at half-height of the exotherm peak,  $\Delta w$ .

## Results and discussion

Compounding polymers with different fillers is a rather simple way to produce new polymer materials with the desired properties. The structure-mechanical properties relationships of multicomponent polymer-matrix composites were mostly investigated as the dependence of particular mechanical property on the contents, properties and interactions of components. The most important mechanical properties: tensile, flexural and impact strength, fracture behaviour (modes, mechanisms, microstructure, toughening) and failure,<sup>3</sup> were usually studied as function of filler particle properties: shape (aspect ratio), size, modulus, surface properties (morphology, roughness/porosity, reactivity, hydrophobicity/hydrophilicity, surface energy and charge), and as filler content.<sup>2-6</sup> Special investigation interests of polymer composites and blends concerned generalized models describing tensile properties as well as fracture and toughening mechanisms.<sup>3</sup> Significantly fewer investigations of these materials concern the restructuring of semicrystalline polymer matrix from microstructural (inner phase structure) to supermolecular level (morphology) of matrix and polymer blends by introduction of filler.<sup>2-5</sup> These papers usually observe the restructuring of polymer matrix as a function of nucleation effect<sup>3,8,9</sup> neglecting other crystallization effects and influencing factors like solidification, viscosity, interfacial properties, steric characteristics, particles orientation, etc.

### Phase structure of the iPP matrix

Semicrystalline isotactic polypropylene (iPP) is a polymorphic material with several crystal modifications including (a) monoclinic  $\alpha$ -iPP phase, (b) trigonal  $\beta$ -iPP phase, (c) orthorhombic  $\gamma$ -iPP phase, and (d) mesostructural smectic iPP phase.<sup>14,15</sup> While most commonly observed  $\alpha$ -iPP crystalline form is stable, the  $\beta$ -iPP phase is metastable and is usually generated at higher undercooling or by inclusion of a nucleating agent (acids and their salts usually are  $\beta$ -nucleators). Fujiyama has firstly shown (1995) that the  $\beta$ -iPP (nucleated by  $\gamma$ -quinacridone) exhibited significantly higher impact strength than stable  $\alpha$ -iPP phase.<sup>16</sup> This difference could not arise from different macromolecules length (strong influencing toughening factor) because the iPP in tested samples, originated from the same type of polypropylene, have the same molecular weight. Higher toughness of the  $\beta$ -iPP could not be explained either by strength of different packed 3/1 helical iPP macromolecules into crystallites. Li et al.<sup>17</sup> finally explained higher toughness of the  $\beta$ -iPP phase with primitive sheaf-like spherulites, characteristic for the  $\beta$ -iPP, in which the spreading of microcrazes are restricted in the directions along the axes of lamellar sheaf.

Incorporated fillers and elastomers may also act as nucleators in the iPP matrix. Plain iPP in WAXD diffractogram usually reveals typical monoclinic  $\alpha$ -iPP phase. WAXD diffractograms of investigated iPP composites and blends reveal strong  $\beta$ -iPP nucleating ability of SEP diblock copolymer<sup>18-21</sup> and wollastonite filler<sup>5,22-24</sup> (appearance of  $\beta$ -300 reflection in diffractogram), as well as strong  $\beta$ -iPP nucleating ability of talc.<sup>4,25,26</sup> Other added components in investigated samples did not seem to show any specified nucleating ability. The WAXD diffractogram of the iPP-1/SEP blend in Figure 1 reveals  $\beta$ -300 reflection proving thus  $\beta$ -iPP nucleating ability of SEP elastomer. This  $\beta$ -300 reflection disappears by introducing talc (T-3) indicating thus supremacy of talc as an  $\beta$ -iPP nucleating agent (Figure 1).<sup>25</sup> Although wollastonite is also known as a strong  $\beta$ -nucleator for the iPP,<sup>27</sup> relatively low content of  $\beta$ -iPP phase (with  $B$  or  $K$  values for measuring  $\beta$ -form

content being 0.02-0.06) in the iPP/W composites was observed (Figure 2)<sup>23</sup> in comparison to literature data<sup>27</sup> ( $K=0.14$  for composite with 3.2 % of wollastonite). Somewhat lower  $\beta$ -form content in the iPP composites with SEBS-*g*-MA than SEBS elastomer might arise from (i) promoting  $\alpha$ -nucleation in the iPP matrix by SEBS copolymer,<sup>28</sup> and/or (ii) from better encapsulation of wollastonite particles by SEBS-*g*-MA than SEBS elastomer that reduces contact with iPP melt and consequently nucleation of  $\beta$ -form (proved by TEM,<sup>23</sup> see *Core-shell morphology of composites*). Although the  $\beta$ -iPP content in iPP/W composites and blends is rather low, it may affect the notched impact strength of the iPP composites and blends in addition to (i) toughening effect of added elastomers and (ii) their ability to affect phase morphology by controlling their molecular properties (for example viscosity).<sup>5, 18-21, 25, 26, 29-31</sup>

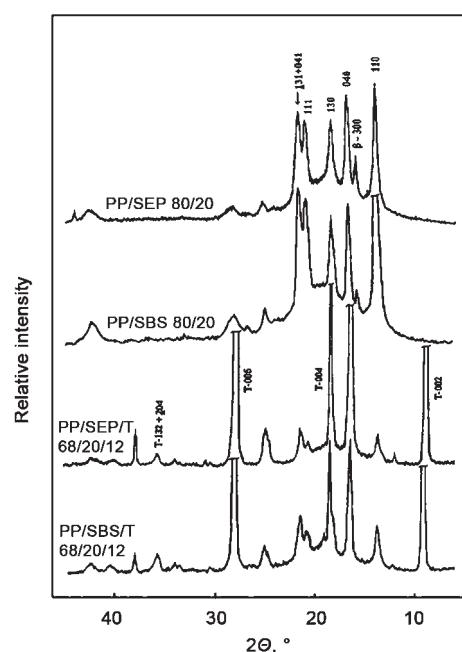


FIGURE 1 - WAXD diffractograms of the iPP-1/T-3/SRBC composites<sup>25</sup>

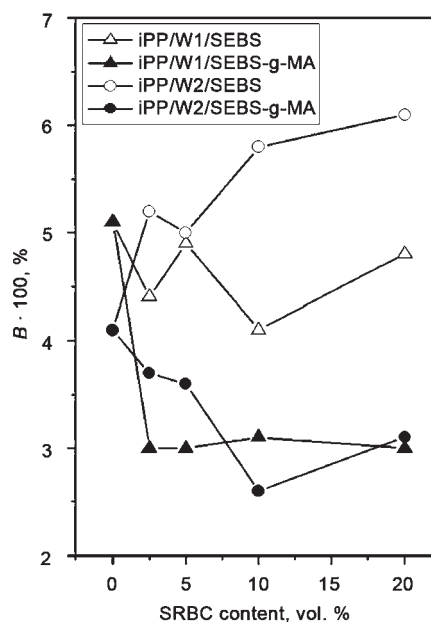


FIGURE 2 -  $B$  parameter (as a measure for  $\beta$ -iPP phase content) of iPP-2/W/SRBC composites as a function of SRBC content<sup>23</sup>

The changes in chemical constitution of the iPP macromolecules might arise during preparation from melt (thermo-oxidative degradation) and by introducing fillers and elastomers in the iPP matrix (interactivity). Recent investigation of thermal degradation of polypropylene has shown that thermo-oxidative degradation of the iPP chains of the iPP samples at higher temperature could be observed by FTIR only at longer exposure (4 day and more) at higher temperature.<sup>32</sup> In the present case the samples (plain iPP, blends and composites) were prepared under the same conditions with short time in melt stage. Moreover, monitoring of specimens by Fourier transformation infrared spectroscopy (FTIR) did not indicate any change in chemical constitution of the iPP chains by introduction of talc and elastomers in the iPP matrix.<sup>33,34</sup> FTIR spectra confirm only the presence of functional groups (hydroxide from talc (hydrogen bond), amide, weak anhydride doublet of SEBS-g-MA) which may interact and/or even react with each other, resulting in formation of imide group between the filler and the elastomer. Moreover, FTIR spectra of iPP/SEBS-g-MA blends and iPP-1/T composites do not indicate chemical change by irradiation of these samples with sterilization dose of 25 kGy.<sup>33,34</sup> Oxidative degradation during irradiation of specimens could not be proved due to the absence of carbonyl, hydroxyl and hydroperoxide peaks. It could be the result of stabilizing effect of SEBS-g-MA and talc in the blends and composites and observable change could be expected at higher irradiation dose. Negligible changes in chemical constitution of the iPP chains may affect defects, but could not affect the structuring of the iPP matrix and gross morphology. Generally, it could be concluded that the phase structure of the iPP matrix was affected by incorporated fillers and polymers prevailing by the *nucleation effect*.

### Crystallite size and crystallinity

The addition of fillers (talc, wollastonite) and elastomers (SRBC, EPDM, mEPR) to the iPP matrix affects crystallite and spherulite size in binary and ternary iPP composites by different effects. While the elastomers may affect the crystallite and spherulite size in the iPP matrix by different effects (i) *nucleation effect*, (ii) *solidification effect*, and (iii) *steric hindrance factors*,<sup>18-21</sup> fillers affect crystallite and spherulite size presumably by nucleation, supercooling effects and steric hindrance effects.<sup>5,23,24</sup>

Smaller dispersed particles of elastomers as well as filler particles can act as heterogeneous nuclei in crystallization process of iPP matrix increasing, thus, heterogeneous nuclei density and decreasing crystallite and spherulite sizes. This effect was observed predominantly in blends as the crystallite size  $L_{040}$  behaviour of the iPP/EPDM blends illustrated in Figure 3.<sup>22</sup> The increase of crystallite size  $L_{040}$  with further EPDM elastomer addition might be ascribed to the prevalence of solidification effect. The crystallization of the iPP matrix during solidification of blends is prolonged and enhanced due to the enabled migration/transfer of iPP chains from the remaining melt islands of elastomers (EPDM in Figure 3)<sup>22</sup> and even partial miscibility or cocrystallizability in the case of the iPP/mEPR blends (second stage).<sup>24</sup> Further addition of elastomer and/or filler may slow down diffusion and crystallization (decreasing crystallite thickening) and sterically hinders regular spherulitization (third stage).

In ternary iPP composites the increase of crystallite size by introducing small filler amounts and slight steady increase with addition of elastomers could be observed (Figures 3 and 4). Increased crystal thickening by incorporation of talc and wollastonite fillers into iPP matrix could be ascribed to the decreased supercooling ( $\Delta T = T_m - T_c$ ) as Figure 5 illustrates this effect for the iPP-2/W/mEPR composites.<sup>24</sup> Such increase of crystallization temperature with filler addition were also reported for the iPP composites with talc and calcium carbonate.<sup>35</sup> The addition of small mEPR amount to the iPP/W composites additionally increases the crystallization temperature (Figure 5). Therefore, the crystallization of the iPP begins at higher temperature and prolongs overall crystallization of the iPP matrix increasing thus crystallite size.<sup>23,24</sup> Such decrease of supercooling

(increase of  $T_c$  values) may be also correlated with the increase of  $\beta$ -iPP phase content nucleated by wollastonite.<sup>23</sup> This fact is in good agreement with the finding of Fujiyama that the crystallization temperature increases with an increase in  $\beta$ -iPP content.<sup>16</sup>

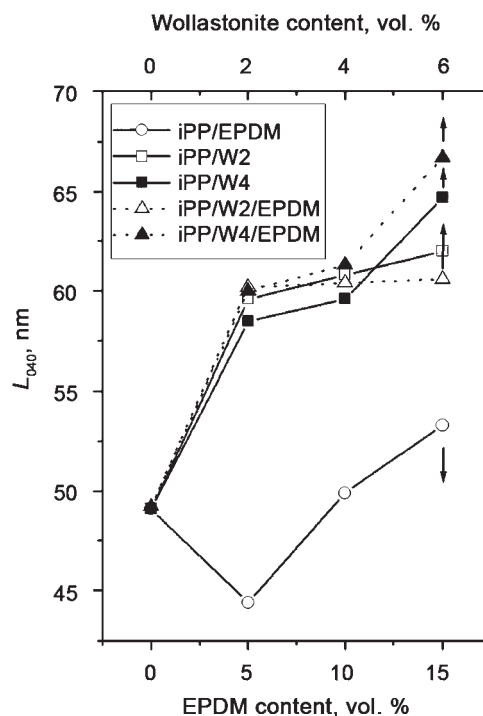


FIGURE 3  $L_{040}$  crystallite size of the iPP-1/W/EPDM composites in dependence of EPDM and wollastonite contents<sup>22</sup>

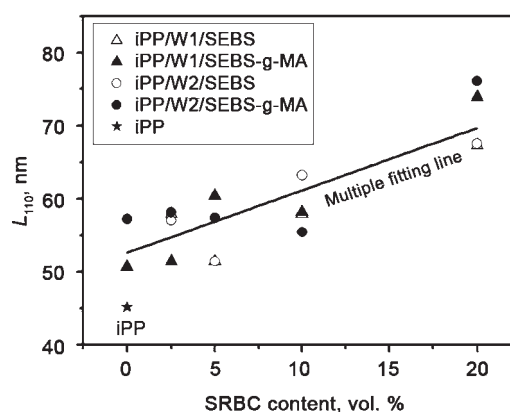


FIGURE 4 -  $L_{110}$  crystallite size of the iPP-1/W/SRBC composites in dependence of SRBC content<sup>23</sup>

Accordingly, in ternary iPP/W/elastomer composites<sup>23,24</sup> slow, but steady, increase of crystallite size with addition of elastomeric component could be observed in Figure 4. Nevertheless, how filler and elastomer affect the crystallite size of the iPP in constitutive binary blends and composites, crystallite size behaviour of ternary iPP composites could not be presented by simple linear combination of constitutive binary systems.<sup>23,24,26</sup> The spherulite growth behaviour of the iPP matrix may differ from crystallite growth because it is governed additionally by factors at gross supermolecular level (see *Structuring of the iPP matrix*).

The degree of crystallinity was determined from WAXD and/or DSC measurements. The overall degree of crystallinity has been calculated as overall crystalline fraction ( $\alpha$ -plus  $\beta$ -iPP phase) in total

polymer fraction (iPP and elastomer) in ternary composite following the Hermans-Weidinger method.<sup>10</sup> The crystallinity values obtained from WAXD measurements are also recalculated on the pure iPP in order to compare them with those obtained from DSC measurements (enthalpy of fusion). The behaviors of crystallinity determined by these two techniques (WAXD and DSC) have the same trend. The degree of crystallinity (Figure 6) shows similar change with the introduction of fillers and elastomers to the change of crystallite size (Figure 4). Somewhat higher increase of crystallinity values was observed by introducing wollastonite into the iPP matrix.<sup>23,24</sup> The addition of elastomers (SBC and mEPR) to the iPP/W composites increases slightly, but steadily the crystallinity values as shown by multiple fitting line in Figure 6.<sup>24</sup> Although wollastonite, as a  $\beta$ -nucleator, contributes to the formation of crystalline  $\beta$ -iPP phase on the account of amorphous iPP phase, the increase of crystallinity with the increasing elastomer content could be explained by several additional effects, (i) enhanced or prolonged crystallization due to solidification effect of SRBC elastomer or even partial miscibility with mEPR elastomer, (ii) dissolution of amorphous iPP, SRBC and mEPR phases by wollastonite and, (iii) limiting resolution of applied methods (WAXD, DSC).

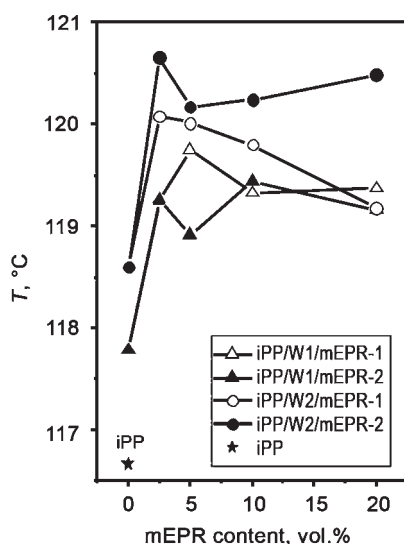


FIGURE 5 - Crystallization temperature ( $T_c$ ) as a function of mEPR content<sup>24</sup>

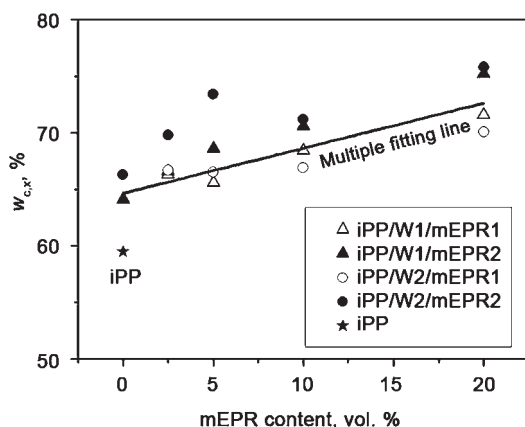


FIGURE 6 - Overall degree of crystallinity,  $w_{c,x}$ , of composites recalculated on the iPP-2 polypropylene mass unit as a function of the mEPR content

### Orientation of filler particles and iPP crystallites

Preparation of the iPP composites with plate-like talc<sup>4,25, 26</sup> or acicular wollastonite fillers<sup>5,22-24</sup> by compression moulding may lead to the preferential orientation of these particles in melt. Fujiyama<sup>36</sup> found that plate-like talc particles aligned parallel to the injection moulding surface affect preferential b-axis alignment perpendicular to the surface of injection moulding. The results of WAXD and different microscopic methods have also proven preferential orientation of talc and wollastonite particles plane-parallel to the compression moulding surface<sup>4,5,22-26,30,31</sup> as was illustrated on SEM micrograph of the iPP/talc/SEBS 78/12/10 composite (Figure 7).<sup>26</sup> Especially high preferential plane-parallel orientation of talc particles, resembling intercalation morphology of polymer nanocomposites, seems to contribute to the mechanical properties and radiation stability of iPP/talc composites.<sup>33,34,37-41</sup> Among all the used SRBC, EPDM and mEPR elastomers only SBS and SEBS-*g*-MA elastomers disorientate plane-parallel talc and wollastonite particles as optical micrograph of the iPP-2/W-2 92/8 composite with 20 vol. % of SEBS-*g*-MA illustrated in Figure 8a.<sup>23</sup> In contrast to the composites with talc and wollastonite particles disoriented by encapsulation with SEBS-*g*-MA (or SBS), plane-parallel orientations of talc and wollastonite particles in ternary iPP composites with SEP, SEBS, EPDM and mEPR were affected negligible. Therefore, Figure 8b for iPP-2/W-2/mEPR-2 composites presents unaffected plane-parallel orientation of wollastonite particles by adding of mEPR elastomer.<sup>24</sup> Plane-parallel orientations of talc and wollastonite particles were proven by changing of reflections intensity ratios calculated from WAXD diffractograms of ternary iPP composites in comparison to the binary iPP/T and iPP/W composites and to plain talc and wollastonite components. The change of intensity ratio of the corresponding reflections of talc and wollastonite crystal phases in these systems with SBS and SEBS-*g*-MA has proven strong disorientation effect of the SEBS-*g*-MA elastomer as shown in Figure 9 for the iPP-1/T-3/SRBC composites.<sup>26</sup>

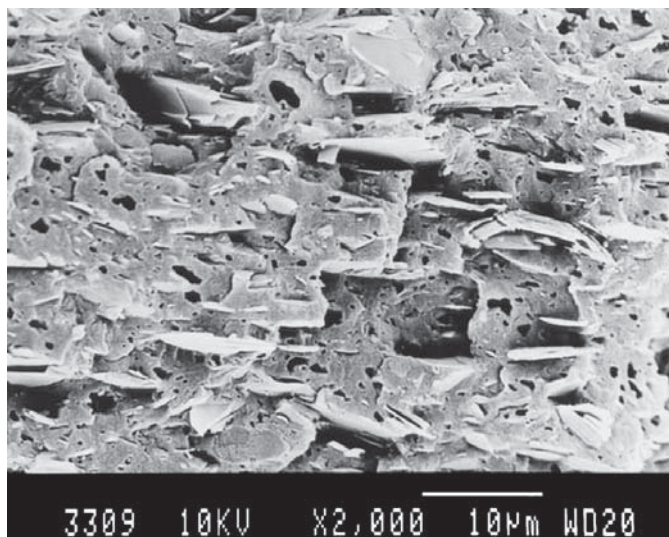


FIGURE 7 - SEM micrographs of xylene etched iPP-1/T-3/SEBS 78/12/10 composite<sup>26</sup>

The incorporation of talc and wollastonite particles as well as the addition of SRBC and mEPR elastomers to the plain iPP and to binary iPP composites may affect the orientational growth of the  $\alpha$ -iPP crystallites. The addition of filler particles to plain iPP, especially plate-like talc, affect orientational growth of  $\alpha$ -iPP crystallites more significantly than the addition of elastomers to the iPP.<sup>22-26</sup> Figure 10 illustratively shows gradually change of C values from 0.235 for iPP-1 up to 0.915 for iPP-1/T-3 88/22 composites due to significant intensity increase of the 040  $\alpha$ -iPP reflection.<sup>26</sup> Only the addition

of SBS and especially SEBS-g-MA to the composites depresses the intensity of 040  $\alpha$ -iPP reflection (Figure 10), whereas SEP, SEBS and mEPR elastomers affect C index negligibly. Obviously, just polar/reactive SBS and SEBS-g-MA elastomers are able to encapsulate and disorientate talc<sup>25,26</sup> and wollastonite<sup>23</sup> particles as was proven by optical, SEM and TEM microscopy (see *Core-shell morphology of composites*) and, in this way, disorientate  $\alpha$ -iPP crystallites. Simultaneously, disorientation of talc and wollastonite particles by their encapsulation with SEBS-g-MA elastomer and disorientation of  $\alpha$ -iPP crystallites (decrease of C values) implies the influence of filler particles on orientational crystallization of the  $\alpha$ -iPP crystallites. High C values in iPP-1/T-3 88/22 composites presume high number of (040) planes in planes plane-parallel to the sample surface, and according to Zipper et al.,  $C = 1$  corresponds to pure  $a^*$ -axis orientation.<sup>13</sup> Lovinger revealed that  $a^*$ -axis is the axial direction of lamellar growth and preferred radial growth of spherulites.<sup>42</sup> Moreover, Fujiyama et al.<sup>43</sup> showed that  $a^*$ -axis-oriented lamellae are parallel to the sample surface. Obviously, plane-parallel accommodated talc crystals affect the growth of plane-parallel  $a^*$ -axis orientation of the  $\alpha$ -iPP lamellae. These results may also suppose some kind of transcrystal growth to the sample surface. Disorientated encapsulated talc particles either affect isotropical growth of the  $\alpha$ -iPP crystallites or they are not able to affect orientational growth of the  $\alpha$ -iPP crystallites any more.

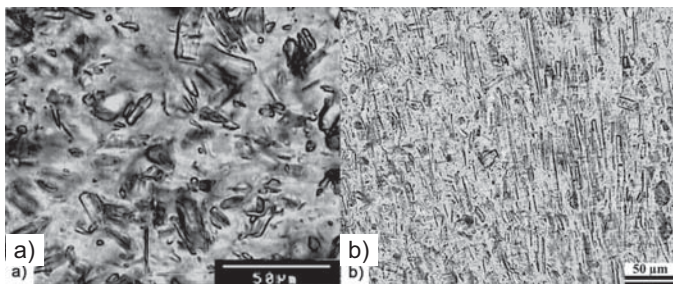


FIGURE 8 - Optical micrographs of (a) iPP-2/W-2/SEBS-g-MA (92/8 + 20) composite,<sup>23</sup> and (b) iPP-2/W-2/mEPR2 (92/8 + 20) composite<sup>24</sup>

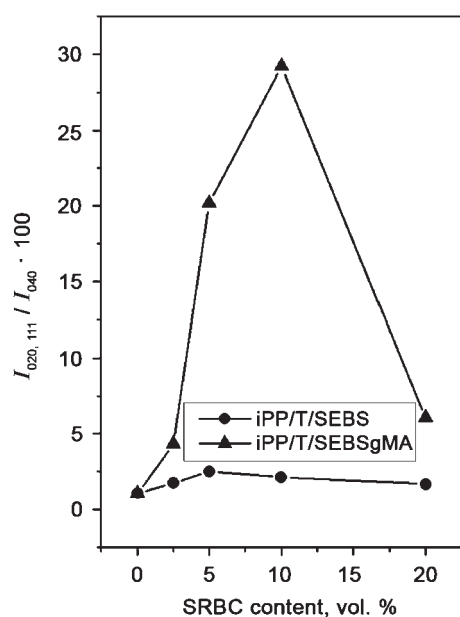


FIGURE 9 - Intensity ratio  $I_{020,111} / I_{004}$  of corresponding talc reflections in dependence on SRBC elastomer added to the iPP-1/T-3 88/12 composites<sup>26</sup>

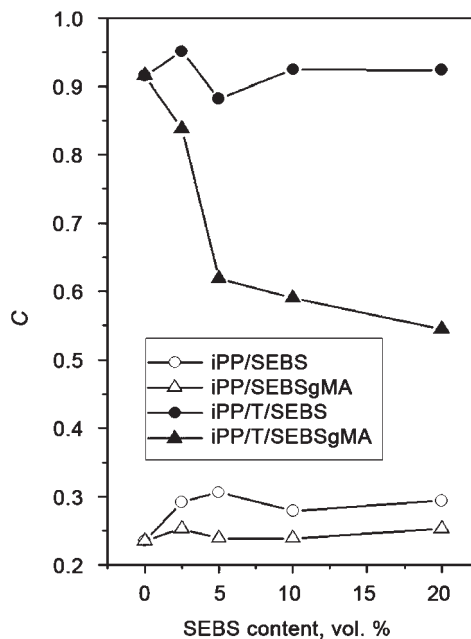


FIGURE 10 - Dependence of orientation parameter C of the iPP-1/SRBC blends and iPP-1/T-3/SRBC composites on elastomer content<sup>26</sup>

### Phase morphology

Previous chapters concern the effects of influencing factors (nucleation, solidification, viscosity, interfacial properties, particles orientation, etc.) on crystallization of polypropylene matrix, e.g. crystallite parameters. In order to complete the structuring picture of ternary polypropylene composites it is important to present gross morphology of polypropylene composites, i.e. it is necessary to investigate the structuring of dispersed elastomer and filler particles in the iPP matrix (arising separated, core-shell or combined morphology) as well as the structuring of the bare iPP matrix (spherulitization).

#### Core-shell morphology of composites

Ternary polymer-matrix composites exhibit two typical microphase morphologies with respect to location of filler and elastomer particles to each other in polymer matrix:<sup>44</sup> (i) *separated microphase morphology* where elastomer and filler particles are randomly separated in polymer matrix, and (ii) *core-shell morphology* where the filler particles are encapsulated by the elastomer. However, the most frequent morphology observed for various composites consists of a combination of two main morphologies.<sup>44</sup> Ternary polymer composites containing core-shell morphology always give better mechanical performance than these ones with separated morphology.<sup>3</sup> The formation of *core-shell morphology* in composites depends on encapsulation ability of elastomers used as impact modifiers and compatibilizing coupling agents simultaneously. Elastomer as an effective compatibilizer encapsulates filler particle with layer, improves the adhesion between filler particle (talc, wollastonite) and matrix phase (iPP), and enables to transfer and withstand the stress and strains caused by an applied load. Effectiveness of compatibilizer coupling agent is very much dependent on different structural characteristics of used copolymer, and the mode of the compatibilizer addition.

Only few authors have reported researches about *core-shell morphology* in ternary composites.<sup>45-48</sup> They found that *core-shell morphology* is influenced by (i) processing conditions during the preparation of the composites<sup>45</sup> and (ii) polar/unsaturated elasto-

mers.<sup>46, 47</sup> Stamhuis presumed that unsaturated elastomers (SBS, SIS) are able to form core-shell morphology in distinction to the saturated elastomers (EPDM, mEPR, SEBS).<sup>46</sup> Stricker et al.<sup>47</sup> confirmed this presumption by finding that polar SEBS-*g*-MA is able to encapsulate talc in the iPP/talc composites in comparison to saturated SEBS elastomer. Our investigations of ternary iPP/talc and iPP/wollastonite composites with SRBC, EPDM and mEPR elastomers proved higher encapsulation efficiency of polar SEBS-*g*-MA and unsaturated SBS compared to other elastomers by optical, SEM and TEM microscopy.<sup>4,5,22-26</sup> SEM micrographs in Figure 11 show the difference in encapsulation ability between SEBS and SEBS-*g*-MA elastomers in ternary iPP/talc/SRBC composites. Although observed morphologies of both composites are the most frequent morphology consisting of a combination of *separated* and *core-shell* morphology, there is evident difference between phase morphology of these ternary composites. In iPP/talc/SEBS composites the dominating role is in separated morphology with randomly distributed SEBS particles (left SEM micrograph), whereas dispersed SEBS-*g*-MA particles are more often located on the talc surface in the iPP/talc/SEBS-*g*-MA composites (right SEM micrograph). Talc particles are partially or completely encapsulated by white, diffuse SEBS-*g*-MA layer, forming thus *core-shell morphology*. More illustrative TEM micrographs in Figure 12 confirm superior encapsulation of wollastonite particles by SEBS-*g*-MA elastomers in comparison to SEBS and mEPR elastomers. While the iPP/W/mEPR composites (iPP-2/W-2/mEPR-1 composite in Figure 12a)<sup>24</sup> exhibit *separated microphase morphology* with randomly dispersed mEPR and wollastonite particles in the iPP matrix, composites iPP/W/SEBS (micrograph of iPP-2/W-2/SEBS composite in Figure 12b)<sup>23</sup> show a variety of morphologies from the mainly separated morphology, over frequently wollastonite particles accommodated alongside SEBS particles in the iPP matrix, to those partly or completely encapsulated by SEBS (insert micrograph in Figure 12b). Moreover, TEM micrographs of composites with SEBS-*g*-MA reveal a greater number of wollastonite particles partly or completely encapsulated by SEBS-*g*-MA elastomer as shown in Figure 12c for the iPP/W-2/SEBS-*g*-MA composite,<sup>23</sup> i.e. the variety of morphologies is shifted to higher extent of *core-shell morphology* also visible in optical micrograph in Figure 8a. Thereby, encapsulation ability of elastomers increases in the following progression mEPR < SEBS < SEBS-*g*-MA.

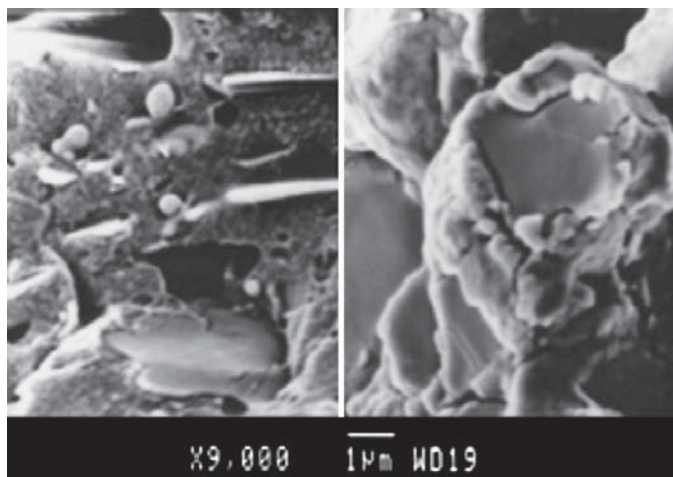


FIGURE 11 - SEM micrographs of unetched composites; iPP-1/T-3/SEBS 78/12/10 (left), and iPP-1/T-3/SEBS-*g*-MA 78/12/10 (right)

Similarly, SBS elastomer exhibited stronger encapsulation of talc than SEP elastomer.<sup>25</sup> Although the surface of some talc and wollastonite fillers was treated with silanes or even alkylsilanes as coupling agents, the interaction or mixing of mEPRs and SEBS with alkyl chains in coupling agents was disabled. The results

based on contact angle measurements also confirm the strongest SEBS-*g*-MA-wollastonite interactions.<sup>5, 23</sup>

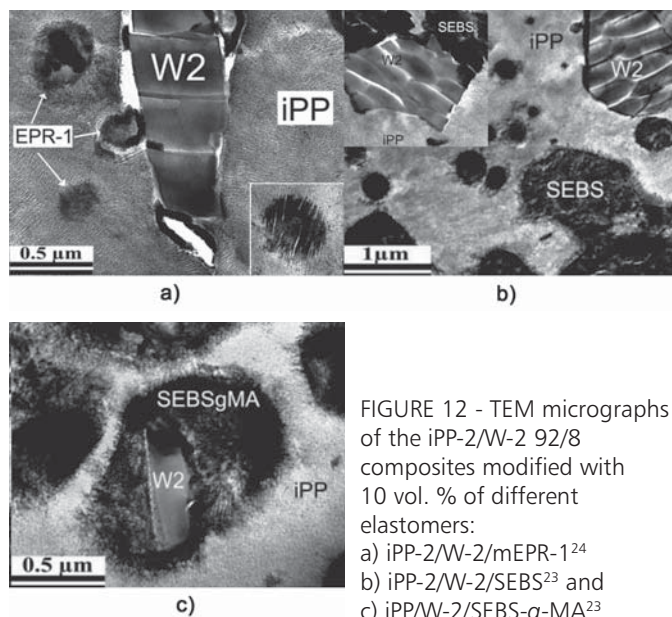


FIGURE 12 - TEM micrographs of the iPP-2/W-2 92/8 composites modified with 10 vol. % of different elastomers:  
a) iPP-2/W-2/mEPR-1<sup>24</sup>  
b) iPP-2/W-2/SEBS<sup>23</sup> and  
c) iPP-2/W-2/SEBS-*g*-MA<sup>23</sup>

#### Structuring of the iPP matrix

The structuring of supermolecular structure of the iPP matrix by introduction of fillers and elastomers depends on different factors from nucleation ability of components to the sterical factors owing to particles morphology and ingredient contents. Among many different supermolecular formations (cylindrites, hedrites, quadrites, dendrites, fibrous crystals, transcristals) of polymers crystallized from melt the most frequent are spherulites.<sup>14,15,49</sup>

Polarization micrographs of compression-moulded plain iPP in investigated iPP systems usually reveal well-developed spherulitic morphology with radial spherulites in polygonal, flower-like or even irregular forms (type I of  $\alpha$ -iPP)<sup>14,15</sup>, and rarely included  $\beta$ -iPP spherulites type III<sup>14,15</sup> in blends and composites with  $\beta$ -iPP phase. The micrograph of neat iPP presented in Figure 13a reveals typically uniform, well-developed spherulitic morphology with radial, polygonal and flower-like spherulites.<sup>24</sup> The incorporation of even very small amounts of both microfillers, talc and wollastonite, in the iPP matrix disturbs the regular spherulitization abruptly. Polarization micrographs of the iPP composites with initial 4 vol. % of plate-like talc particles exhibit thin, dark iPP grains or nodules with curly branches at circumferences and without the Maltese cross under polarization light, even at higher magnification as illustrated by micrograph of iPP-1/T-3 96/4 composite in Figure 13b.<sup>50</sup> Further addition of talc does not change gross morphology as well as the addition of SRBC elastomers.<sup>4,25,26</sup> The incorporation of thin needle-like wollastonite particles into iPP matrix affects regular spherulitization in lower degree than talc leading to the morphology with small irregular spherulites or with thin, dark branched iPP grains without the Maltese cross (Figure 13c).<sup>5,22-24</sup> It was also shown that the spherulites size step-wise decreased to approximately half with low addition of 2 vol. % wollastonite; gradual decrease and disturbance of spherulites occur with the increasing content of all wollastonite types (up to 16 vol. %).<sup>5</sup> In most iPP/W composites the spherulites were still recognizable up to 8 vol. % of wollastonite content as shown in the micrograph in Figure 13c.<sup>24</sup> It seems that plate-like talc and thin needle-like wollastonite particles strongly affect the spherulitization of the iPP matrix by *nucleation effect*. However, the differences of disturbance efficiency in spherulitization of the iPP matrix between these two fillers indicate possible additional effect of *sterical hindrances* on the iPP morphology. Namely, according to Burke et al.<sup>51</sup> the spherulite growth may be also restrained by steric hindrances at filler particles surface. This effect seems to be similar

to *sterical hindrance effect* of enlarged dispersed polystyrene and SBS particles in the iPP matrix that transform the well-developed spherulitic morphology above critical dispersed particle size into morphology with cross-hatched bundles of sandwich lamellae.<sup>52</sup>

The addition of elastomers to the binary iPP/T and iPP/W composites may change the filler particles orientation (Figures 8a, 9), size (Figures 3, 4) and orientation of the iPP crystalites (Figure 10) affected by fillers particles so far as elastomers are capable to encapsulate fillers particles and form *core-shell morphology* (Figures 11, 12). Apart from that, added elastomers may affect the structuring of the iPP matrix by competitive nucleation, solidification and steric hindrance effects. Due to appreciable similarity of the iPP matrix with propylene-based metallocene copolymers (mEPRs) and EPDM, the addition of higher amounts of EPDM or mEPR elastomers to the iPP composites may affect crystallization of the iPP matrix by renewing and enlarging the iPP spherulites in the iPP/W composites (Figure 13 d).<sup>22,24</sup> Competitive solidification (increase of spherulite size up to 10 vol. % of EPDM) and steric hindrance (decrease of spherulite size at higher contents) effects could be recognized from the spherulite size curves of the iPP/W/EPDM composites presented in Figure 14.<sup>22</sup> The effect of EPDM addition to the iPP/W-2 composites seems to be similar to this effect for the iPP/EPDM blends but at lower level. The addition of EPDM to the iPP/W-4 composites seems to show even steady increase (Figure 14). It seems that chemical similarity (iPP with mEPR and EPDM), as well as prolonged crystallization due to *solidification effect* by added elastomers counteract to the *nucleation and steric hindrance effect* of wollastonite. The inserted figure in Figure 12a reveals the protrusion of the iPP lamellae through the spherical mEPR particles. This could be a result of good compatibility or even co-crystallizability of dispersed mEPR particles with iPP matrix.<sup>22, 24</sup>

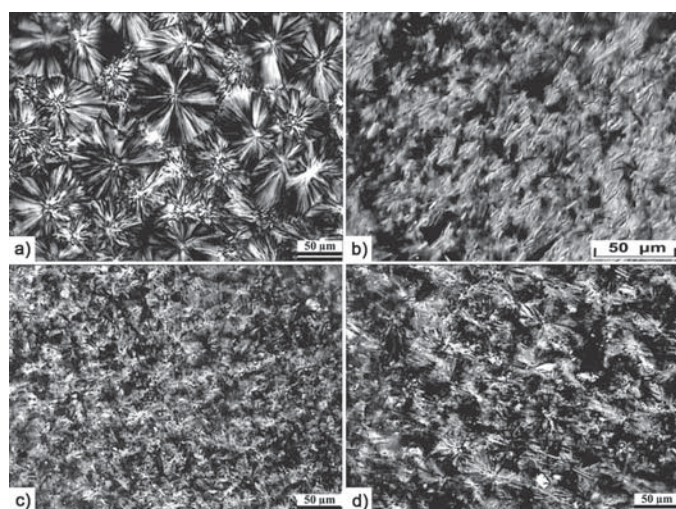


FIGURE 13 - Polarization micrographs of a) plain iPP-2,<sup>24</sup> b) iPP-1/T-3 96/4,<sup>50</sup> c) iPP-2/W-2 92/8,<sup>24</sup> d) iPP-2/W-2 92/8 + 20 % mEPR-1<sup>24</sup>

## Conclusion

From the results obtained by different experimental methods, the following conclusions about factors influencing the structuring of the iPP matrix in binary iPP/T, iPP/W and ternary iPP/T/SRBC, iPP/W/SRBC, iPP/W/EPDM, and iPP/W/mEPR compression moulded composites, as well as in the binary iPP/SRBC, iPP/EPDM, and iPP/mEPR compression moulded blends can be summarized:

*Nucleation* abilities of smaller dispersed and filler particles were dominant at smaller filler and elastomer contents. It manifests in the crystallite and spherulite sizes a decrease due to the increase of heterogeneous nuclei density affected by incorporated particles.

*Plane-parallel orientations* of talc and wollastonite particles in compression moulded composites were changed by adding polar/reactive SBS and SEBS-g-MA elastomers.

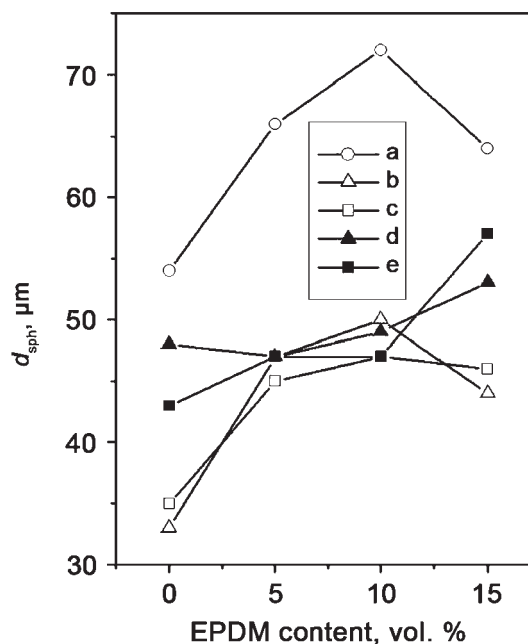


FIGURE 14 - Spherulite diameter as a function of elastomer content for (a) iPP/EPDM blend, and iPP/W-2/EPDM composites<sup>22</sup> with (b) 2 vol.% and (c) 4 vol.% of W2, as well as iPP/W-4/EPDM composites with (d) 2 vol.% and (e) 4 vol.% of W4

*Orientation growth* of the  $\alpha$ -iPP crystallite was significantly affected by incorporation of fillers and reoriented by polar/reactive SBS and SEBS-g-MA elastomers.

Crystallite and spherulite size increased when *solidification effect*, enabling prolonged crystallization with *migration/transferring* of the iPP chains from elastomeric melt islands to growing crystallites/spherulites, prevailed competitive *nucleation effect*.

*Core-shell morphology* of ternary iPP compression moulded composites occurred only in the cases of polar/reactive SBS and SEBS-g-MA elastomers able to encapsulate filler particles.

*Steric hindrance factors* of filler particles may affect the spherulitization of the iPP matrix and final morphologies of compression moulded binary and ternary composites.

Renewing and enlarging the iPP spherulites in the iPP/W composites could be affected by *cocrystallization* in the iPP lamellae protruded through spherical dispersed mEPR particles in addition to *solidification effect* of elastomers mentioned above.

## Acknowledgements

The authors would like to express their gratitude for the *financial support provided by the Ministry of Higher Education, Science and Technology of the Republic of Slovenia and the Ministry of Science, Education and Sports of the Republic of Croatia* (Grant No. 098-0982904-2955). *The authors would also like to thank dipl. ing. J. Pohleven for his help in the experimental work, Dr. E. Ingolič for her valuable help in elaborating TEM micrographs, Dr. M. Leskovac for her valuable elaborations of adhesion properties, and M. Makarovič for his valuable elaborations of mechanical properties data.*

## REFERENCES

- Kietzman, J. H.: *Asbestiform fillers in Additives for Plastics*, Vol 1 (Ed. Seymour, R. B.), New York, Academic Press, 1978., 51-77.
- Rothon, R. N.: *Particulate-Filled Polymer Composites*, 2<sup>nd</sup> edition, Shawbury, Rapra, 2006., 404-406.

3. Wypych G.: *Handbook of fillers*, 2nd edition, Toronto, ChemTec Publishing, 2000.
4. Denac, M.: *Modifikacija izotaktičnega polipropilena s talkom, stirenskimi blokopolimeri in z ionizacijskim obsevanjem*, Ph.D. Thesis; University of Maribor, Maribor, Slovenia, 2004.
5. Švab, I.: *Študij modifikacije izotaktičnega polipropilena z wollastonitom in elastomeri*, Ph.D. Thesis, University of Maribor, Maribor, Slovenia, 2006.
6. Pukanszky, B.: *Polyolefin Composites: Interfacial Phenomena and Properties in Handbook of Polyolefins*, 2nd edition, (Vasile, C.; ed.), New York, Marcel Dekker, 2000., 689-722.
7. Pukanszky, B., Maurer, F. H. J.: *Composition dependence of the fracture toughness of heterogeneous polymer systems*, *Polymer*, 36(1995), 1617-1625.
8. Bartczak, Z., Martuscelli, E., Galeski, A.: *Primary spherulite nucleation in polypropylene-based blends and copolymers*. In *Polypropylene: Structure blends and composites*, Vol. 2: *Copolymers and Blends*. Ch 2. (Ed. Karger-Kocsis. J.) London, Chapman and Hall, 1995.
9. Long Y., Shanks R.A., Stachurski Z.H.: *Kinetics of polymer crystallisation*. *Prog. Polym. Sci.* 20(1995), 651-701.
10. Weidinger, A., Hermans, P.H.: *On the Determination of the Crystalline Fraction of Isotactic Polypropylene from X-Ray Diffraction*, *Makromol. Chem.*, 50(1961), 98-115.
11. Alexander L. E.: *X-ray diffraction methods in polymer science*, New York, John Wiley, 1969., Ch 7, 423-466.
12. Turner-Jones, A., Aizlewood, J. M., Beckett, D. R.: *Crystalline Forms of Isotactic Polypropylene*. *Makromol. Chem.*, 75(1964), 134-154.
13. Zipper, P., Janosi, A., Wrentschur, E.: *Scanning X-ray scattering of mouldings from semicrystalline polymers*, *J. Physique IV, Suppl. J. Phys. I* 3(1993), 33 - 36.
14. Padden, F.J., Keith, H.D.: *Spherulitic Crystallization in Polypropylene*, *J. Appl. Phys.*, 30(1959), 1479-1484.
15. Varga J.: *Supermolecular structure of isotactic polypropylene*, *J. Mater. Sci.*, 27(1992), 2557-2579.
16. Fujiyama, M.: *Structures and Properties of Injection Moldings of  $\beta$ -Crystal Nucleator-Added Polypropylenes Part 1 Effect of  $\beta$ -Crystal Nucleator Content*, *Intern. Polym. Process.*, 10(1995), 172-178.
17. Li, J X., Cheung, W. L., Chan, C. M.: *On deformation mechanisms of b-polypropylene 3. Lamella structures after necking and cold drawing*, *Polymer* 40(1999), 3641-3656.
18. Radonjič, G.: *Kompatibilizacija mešanice polipropilena in polistirena z blokopolimeri*, PhD Thesis; University of Maribor, Maribor, Slovenia, 1998.
19. Radonjič G., Šmit I.: *Phase morphology and mechanical properties of iPP/SEP blends*. *J. Polym. Sci. Part B: Polym. Phys.*, 39(2001), 566-580.
20. Radonjič, G., Šmit, I.: *Modifikacija izotaktičnega polipropilena z blokopolimerom SEP, Zbornik referatov s posvetovanja: Slovenski kemijski dnevi 2002* (Eds. Glavič, P., Brodnjak-Vončina, D.), Maribor, Slovenija, Slovensko kemijsko društvo, 2002., 355-362.
21. Šmit, I., Radonjič, G., Hlavata D.: *Phase morphology of iPP/aPS/SEP blends*, *Eur. Polym. J.*, 40(2004), 1433-1443.
22. Šmit, I., Musil, V., Švab, I.: *Effects of EPDM and Wollastonite on Structure of Isotactic Polypropylene Blends and Composites*, *J. Appl. Polym. Sci.*, 91(2004), 4072-4081.
23. Švab, I. et al. *Phase structure and morphology of wollastonite reinforced polypropylene composites modified with SEBS and SEBS-g-MA elastomers*, *Polym. Eng. Sci.*, 47(2007), 2145-2154.
24. Švab, I. et al. *Wollastonite-reinforced polypropylene composites modified with novel metallocene EPR copolymers. I. Phase structure and morphology*, *Polym. Compos.*, 30(2009)7, 1007-1015.
25. Denac M., Musil V., Šmit I.: *Structure and mechanical properties of talc-filled blends of polypropylene and styrenic block copolymers*. *J. Polym. Sci., Polym. Phys.*, 42(2004), 1255-1264.
26. Denac, M., Šmit, I., Musil, V.: *Polypropylene/talc/SEBS (SEBS-g-MA) composites, Part 1. Structure*, *Compos. A*, 36(2005), 1094-1101.
27. Liu, J., Wei, X., Guo, Q.: *The  $\beta$ -Crystalline Form of Wollastonite-Filled Polypropylene*, *J. Appl. Polym. Sci.*, 41(1990), 2829-2835.
28. Gupta, A. K., Purwar, S. N.: *Crystallization of PP/SEBS Blends and Its Correlation with Tensile Properties*, *J. Appl. Polym. Sci.*, 29(1984), 1595-1609.
29. Švab, I., Musil, V., Leskovic, M.: *The Adhesion Phenomena in Polypropylene/Wollastonite Composites*, *Acta Chim. Slov.*, 52(2005), 264-271.
30. Švab, I. et al.: *Mechanical properties of wollastonite-reinforced polypropylene composites modified with SEBS and SEBS-g-MA elastomers*, *Polym. Eng. Sci.*, 47(2007), 1873-1880.
31. Švab, I. et al.: *Wollastonite-reinforced polypropylene composites modified with novel metallocene EPR copolymers II. Mechanical properties and adhesion*, *Polym. Compos.*, 30(2009)8, 1091-1097.
32. de Goede, S. et al.: *Monitoring Thermo-Oxidative Degradation of Polypropylene by CRYSTAF and SEC-FTIR*, *Macromol. Symp.*, 193(2003), 35-43.
33. Denac, M. et al.: *Effects of talc and gamma irradiation on mechanical properties and morphology of isotactic polypropylene/talc composites*, *Polym. Degradat. Stab.*, 82(2003), 263-270.
34. Denac, M. et al.: *Influence of Talc and SEBS-g-MA on PP/Talc/SEBS-g-MA Composites Under the Gamma Irradiation Sterilization Conditions*, *Macromol. Symp.*, 217(2004), 401-417.
35. Pukanszky, B. et al.: *Effect of nucleation, filler anisotropy and orientation on the properties of PP composites*, *Composites*, 25(1994)3, 205-214.
36. Fujiyama, M.: *Crystal Orientation in Injection Moldings of Talc-filled Polyolefins*, *Intern. Polym. Process.*, 13(1998), 284-290.
37. Denac, M., Musil, V.: *The influence of thermoplastic elastomers on morphological and mechanical properties of PP/talc composites*, *Acta Chim. Slov.*, 66(1999), 55-67.
38. Denac, M. et al.: *Effect of irradiation on tensile properties of modified polypropylenes*, *Proceedings of the 13th IGWT Symposium: Commodity science in global quality perspective: products - technology, quality and environment*, Volume 1 (Denac, M., Musil, V., Pregrad, B. (Eds.)), Maribor, Slovenia, 2001., 377-382
39. Denac, M. et al.: *Vpliv ionizirajočega sevanja na mehanske lastnosti kompozitov PP/talc/SEBS. Zbornik referatov s posvetovanja: Slovenski kemijski dnevi 2001* (Glavič, P., Brodnjak-Vončina, D. (Eds.)), Maribor, Slovenia, 2001., 610-617.
40. Musil, V. et al.: *Modification of isotactic polypropylene with fillers and thermoplastic elastomers*, *Book of Abstract: Euroconference on University and Enterprise* (Chiacchierini, E. (Ed.)), Rim, Italia, Universita La Sapienza, 2002., 823-830.
41. Denac, M., Musil, V., Šmit, I.: *Polypropylene/talc/SEBS (SEBS-g-MA) composites. Part 2. Mechanical properties*, *Compos. A*, 36(2005), 1282-1290.
42. Lovinger A. J.: *Microstructure and Unit-Cell Orientation in  $\alpha$ -Polypropylene*, *J. Polym. Sci., Polym. Phys. Ed.*, 21(1983), 97-110.
43. Fujiyama, M., Wakino, T., Kawasaki, Y.: *Structure of Skin Layer in Injection-Molded Polypropylene*, *J. Appl. Polym. Sci.*, 35(1988), 29-49.
44. Long, Y., Shanks, R. A.: *PP-Elastomer-Filler Hybrids. I. Processing, Microstructure, and Mechanical Properties*, *J. Appl. Polym. Sci.*, 61(1996), 1877-1885.
45. Ou, Y. C. et al.: *Toughening and reinforcing polypropylene with core-shell structured fillers*. *J. Appl. Polym. Sci.*, 74(1999), 2397-2403.
46. Stamhuis, J. E.: *Mechanical properties and morphology of polypropylene composites. Talc-filled, elastomer-modified polypropylene*, *Polym. Compos.*, 5(1984), 202-207.
47. Stricker, F., Mülhaupt R.: *Compatibilized polypropylene hybrid composites: influence of elastomeric interlayers on mechanical properties and nucleation behaviour*, *High. Perform. Polym.*, 8(1996), 97-108.
48. Setz, S. et al.: *Morphology and mechanical properties of blends of isotactic or syndiotactic polypropylene with SEBS block copolymers*, *J. Appl. Polym. Sci.*, 59(1996), 1117-1128.
49. Wunderlich, B.: *Macromolecular Physics, Vol. 1: Crystal Structure, Morphology, Defects*, New York, Academic Press, 1973. Chapter 3, 179-378.
50. Šmit, I., Denac, M., Musil, V.: *Unpublished data*.
51. Burke, M., Young, R.J., Stanford, J.L.: *The spherulitic and lamellar morphology of titanium dioxide-filled polyolefins*, *Plast. Rubber Compos. Process. Appl.*, 20(1993), 121-135.
52. Šmit, I., Radonjič, G.: *Effects of SBS on phase morphology of the iPP/aPS blends*, *Polym. Eng. Sci.*, 40(2000), 2144-2160.

## CONTACT

Dr. sc. Ivan Šmit  
 Ruđer Bošković Institute  
 Bijenička 54  
 HR-10002 Zagreb, Croatia  
 E-mail: ismit@irb.hr